

Supplemental Data

ANALYSIS OF CD44-HYALURONAN INTERACTIONS IN AN ARTIFICIAL MEMBRANE SYSTEM: INSIGHTS INTO THE DISTINCT BINDING PROPERTIES OF HIGH AND LOW MOLECULAR WEIGHT HYALURONAN*

Patricia M. Wolny^{2,1}, Suneale Banerji³, Céline Gounou⁴, Alain R. Brisson⁴, Anthony J. Day⁵, David G. Jackson³ and Ralf P. Richter^{1,2}

From the Biosurfaces Unit¹, CIC biomaGUNE, Paseo Miramon 182, 20009 Donostia-San Sebastian, Spain, the Max-Planck-Institute for Metals Research², Stuttgart, Heisenbergstraße 3, 70569 Stuttgart, Germany, the MRC Human Immunology Unit³, Weatherall Institute of Molecular Medicine, John Radcliffe Hospital, Headington, Oxford OX3 9DS, UK, the Laboratoire d'Imagerie Moléculaire et Nano-Bio-Technologie⁴, IECB, UMR-5248 CBMN, CNRS-Université Bordeaux 1-ENITAB, Avenue des Facultés, 33402 Talence, France, and the Wellcome Trust Centre for Cell Matrix Research⁵, Faculty of Life Sciences, University of Manchester, Oxford Road, Manchester M13 9PT, UK
Running head. *In vitro* model of HA-cell surface interactions

Address correspondence to: Ralf Richter, Biosurfaces Unit, CIC biomaGUNE, Paseo Miramon 182, 20009 Donostia-San Sebastian, Spain.

Phone: +34 943 00 53 29; Fax: +34 943 00 53 15; E-mail: rrichter@cicbiomagune.es

Calibration curves relating QCM-D frequency shifts to surface densities of CD44 HABDs and HA

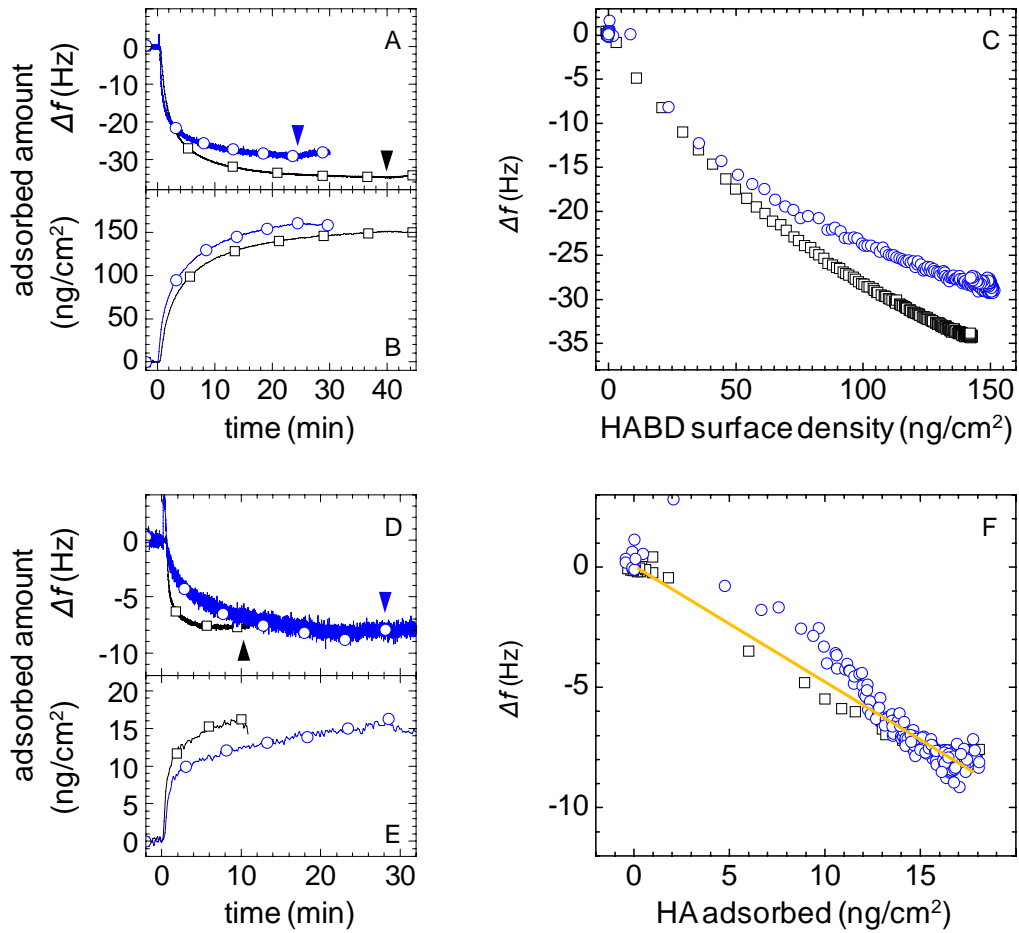


Figure S1. Correlation between the QCM-D frequency shifts upon binding of HABD (A-C) and HA (D-F) and adsorbed amounts, from simultaneous measurements by QCM-D and ellipsometry on the same surface. (A) QCM-D frequency shifts upon incubation of his-HABD (blue line with circles) and (HABD)₂-Fc (black line with squares), respectively. Incubation started at 0 min; rinses in buffer are indicated (arrowheads). (B) Corresponding biomolecular masses as determined by ellipsometry. (C) Parametric plot of the data from (A) and (B). With the aid of these calibration curves, the amount of adsorbed HABD can be quantified from QCM-D frequency shifts for arbitrary coverages (1,2). (D) QCM-D frequency shifts upon exposure of 10 μ g/ml 262 kDa HA to his-HABD (blue line with circles) and (HABD)₂-Fc (black line with squares) coated surfaces, respectively. (E) Corresponding biomolecular masses, measured by ellipsometry. (F) Parametric plot of the data in (D) and (E). A linear approximation of the data (solid orange line) was used to estimate the adsorbed amounts of HA from QCM-D frequency shifts at arbitrary receptor coverages. The molar surface densities of HABD monomers and HA in Fig. 7B were determined from the calibration curves in (C) and (F), respectively, and the molecular weights of his-HABD (39 kDa), (HABD)₂-Fc (2 \times 58 kDa) and HA (262 kDa).

Colloidal probe reflection interference contrast microscopy

This optical microscopic technique measures the height at which a colloidal probe hovers above a transparent planar substrate (3,4). The interference of light that is reflected at the glass-liquid interface and at the colloidal-probe liquid interface, respectively, gives rise to a characteristic intensity pattern of concentric rings (Fig. S2A), from which the height of the bead above the glass substrate can be determined (3,4).

3W-RICM. For the unambiguous determination of distances in the range of several hundred nanometers, simultaneous measurements at several wavelengths are required. We implemented a triple-wavelength RICM (5), inspired by the dual-wavelength approach of Schilling et al. (6).

The setup was based on an inverted microscope (Axio Observer Z1, Zeiss, Oberkochen, Germany). A Xenon lamp (XBO 75, Zeiss) was used as light source. Stray light was filtered by the antireflective technique (4,7), using a filter cube with crossed polarizers (AHF Analysentechnik, Tübingen, Germany) and an antireflective objective (EC Plan Neofluar Antireflective, 63×/1.25, Zeiss). Reflected light was split into three different beams using a custom built beam splitter unit with integrated band pass filters (AHF Analysentechnik) of 10 nm width, centered at 490, 546 and 630 nm, respectively. Images were captured with two cameras (ORCA-ER, Hamamatsu Photonics, Massy, France) simultaneously, using the software SimplePCI (Hamamatsu) and exposure times of typically 100 ms. Interferographs at 490 and 546 nm were acquired by two halves of the chip of one camera. Images at 630 nm were taken with the second camera.

Sample preparation. Cleaned glass cover slips were glued to a custom built Teflon holder using two component silicon glue (Twinsil, Picodent, Wipperfurth, Germany). The assembly defined an open liquid cell (~100 μ l total volume) in which the cover slip served as the bottom of the cell.

SLBs, and layers of AnxA5-Z, (HABD)₂-Fc and HA were prepared on the glass cover slip, following the same incubation steps as those established by QCM-D (Fig. 2). Incubation was performed in still solution, with twofold increased concentrations and incubation times. Samples were injected directly into the buffer-filled liquid cell at desired concentrations. The liquid volume was maintained at about 50 μ l, and homogenized by repeated suction and release of a fraction of the liquid by a pipette. To remove samples, the cell's content was diluted, by repeated addition of at least a twofold excess of buffer, pipette assisted homogenization and removal of excess liquid, until the concentration of soluble sample was below 10 ng/ml. Care was taken that the glass surface remained wet at any time.

Preparation of colloidal probes. Polystyrene microspheres (Polysciences, Eppelheim, Germany) of ~25 μ m diameter were coated with poly(ethylene glycol)-block-(polypropylene glycol)-block-(polyethylene glycol) (PEG-PPG-PEG) with a number averaged molecular weight, $M_n = 8.4$ kDa, and containing 80 weight-% PEG (Pluronic F-68, Sigma). The average size of each PEG block (3.4 kDa, or $N = 76$ monomer units) corresponds to a radius of gyration of 2.2 nm (8), and a contour length of ~30 nm. The method of Kim et al. (9), based on solvent-assisted entrapment of the triblock-copolymer on the particle surface, was adapted for passivation. PEG-PPG-PEG was dissolved in ultrapure water at a concentration of 10 mg/ml. Polystyrene microspheres were added at a concentration of 0.26 mg/ml. This corresponds to a total mass of 160 μ g PEG-PPG-PEG per cm^2 of microsphere surface area. The mixture was stirred for 5 h at room temperature, 45 μ l toluol were added under continued stirring for 2 h, and toluene was removed by evaporation at 98°C for about 15 min. The particle solution was washed repeatedly, by centrifugation and re-dispersion of the pellet in ultrapure water, until a nominal concentration of less than 10 ng/ml PEG-PPG-PEG was reached.

Colloidal probes were added to the liquid cell at concentrations that ensured sparse coverage (~20 microspheres/ mm^2).

Height determination. Interferographs (fig. S2A) were analyzed numerically, using custom developed algorithms implemented in Matlab. The height of the colloidal probe above the glass support was determined with a simple model (parallel plate approximation with incident light parallel to the surface normal) (3), from the radial position of the extremum in the radially averaged interferometric intensity profile that was situated closest to but not closer than 1 μ m from the center. The diameter of the bead was determined from bright field images.

Based on the estimated accuracy in the determination of the bead diameter (± 0.5 μ m) and the focus position (± 0.2 μ m), and the noise in the intensity profile, we estimate the setup-specific variations in the apparent height to be smaller than ± 6 nm. The heights determined from all three wavelengths ($\lambda = 490, 546$ and 630 nm) were usually found to agree within an interval of less than 10 nm.

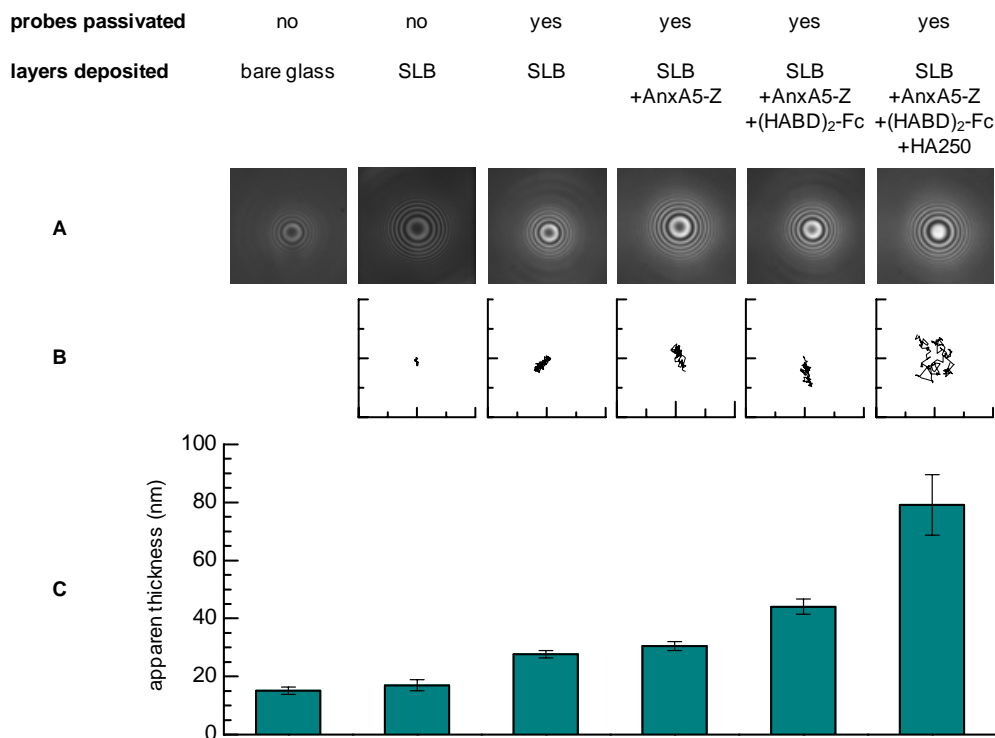


Figure S2. RICM data acquired at different stages (*noted on top*) of the assembly of model system 1. (A) Representative interferographs ($\lambda = 490$ nm, image size $20 \mu\text{m}$), displaying the characteristic pattern of concentric rings (Newtonian rings). The increase in intensity in the center of the pattern, from the leftmost to the rightmost image, reflects the increase in distance between the colloidal probe and the glass substrate. (B) Typical traces of the in-plane movement of a bead's center over a period of 10 s (full scales on the x and y axis correspond to $1 \mu\text{m}$). Non-passivated colloidal probes show no significant in-plane movement on SLBs, i.e., they are immobilized due to strong adsorption. Passivated probes show increasing diffusive motion on SLBs, and films of AnxA5-Z, (HABD)₂-Fc and HA250, indicating little or no attractive interaction with the surface adlayer. (C) Apparent heights. Error bars represent standard deviations from measurements at $\lambda = 490$ nm with 5 to 10 different beads at various positions on the same sample. We found an apparent height of 15 ± 4 nm, instead of 0 nm, for non-passivated probes adsorbed to glass. Most likely, and as discussed in ref. (3), this discrepancy stems from limitations in the accuracy of the simple model. The nanoscale roughness of the probe may though also contribute. Addition of the SLB increased the thickness by only few nanometers, as expected. The increase in height of 11 ± 4 nm for PEG passivated probes on SLBs is likely to reflect the hydrated PEG layer that now separates the bead from the surface. Indeed, a height of around 10 nm would agree with the thickness of a rather dense brush of moderately stretched PEG chains. Upon addition of AnxA5-Z and (HABD)₂-Fc, the height increases by another 16 ± 4 nm. This is similar to the dimensions of the adsorbed biomolecular layer (~ 13 nm). On the HA film, the variations in measured heights were within a range of 15 to 25 nm, which is smaller than the thickness of the HA films. This suggests that the HA film was laterally homogeneous on length scales above the size of the contact area between the bead and the substrate ($\sim 1 \mu\text{m}$).

Influence of interactions between the colloidal probe and the sample on apparent film thickness. Once passivated with PEG, our beads retained mobility on all of the employed samples (Fig. S2B). This indicates that adhesive interactions between bead and sample are small, and therefore unlikely to perturb the sample appreciably. Electrostatic interactions may repel the probe from the surface, but are rather short ranged under the employed conditions: the Debye length is below 1 nm at salt concentrations of 150 mM NaCl. Hence we expected that electrostatics do not affect the measured thickness appreciably.

In addition to these interactions, gravitational forces will press the colloidal probe onto the sample. From the density difference between polystyrene and water (0.055 g/cm^3) and the microsphere's typical radius ($R = 12.5 \mu\text{m}$), this force can be calculated to be $F_g = 4.4 \text{ pN}$, or $F_g/R = 0.35 \mu\text{N/m}$. For comparison, forces of $>1 \text{ mN/m}$ would be required to compress SLBs or any of the employed protein layers appreciably (10). The HA films, however, are likely to be very soft, and may indeed be affected (11,12). The measured HA film thicknesses should therefore be considered lower bounds of the real hydrodynamic film thickness.

References

1. Carton, I., Malinina, L., and Richter, R. P. (submitted)
2. Bingen, P., Wang, G., Steinmetz, N. F., Rodahl, M., and Richter, R. P. (2008) *Anal. Chem.* **80**, 8880-8890
3. Kühner, M., and Sackmann, E. (1996) *Langmuir* **12**, 4866-4876
4. Limozin, L., and Sengupta, K. (2009) *ChemPhysChem* **10**, 2752-2768
5. Richter, R. P., Hock, K. K., Burkhartsmeier, J., Boehm, H., Bingen, P., Wang, G., Steinmetz, N. F., Evans, D. J., and Spatz, J. P. (2007) *J. Am. Chem. Soc.* **129**, 5306-5307
6. Schilling, J., Sengupta, K., Goennenwein, S., Bausch, A. R., and Sackmann, E. (2004) *Phys. Rev. E* **69**, 021901
7. Ploem, J. S. (1975) *Reflection-Contrast Microscopy as a Tool for Investigation of the Attachment of Living Cells to a Glass Surface*, Blackwell Scientific, Oxford
8. Kawagushi, S., Imai, G., Suzuki, J., Miyahara, A., Kitano, T., and Ito, K. (1997) *Polymer* **38**, 2885-2891
9. Kim, A. J., Manoharan, V. N., and Crocker, J. C. (2005) *J. Am. Chem. Soc.* **127**, 1592-1593
10. Israelachvili, J. N. (1992) *Intermolecular and Surface Forces*, 2nd ed., Academic Press Ltd, London
11. Li, F., and Pincet, F. (2007) *Langmuir* **23**, 12541-12548
12. Robert, P., Sengupta, K., Puech, P. H., Bongrand, P., and Limozin, L. (2008) *Biophys. J.* **95**, 3999-4012